Energy Materials

Supplementary Materials

Cellulase-mediated surface engineering of cellulose fibers for high-performance cellulose fibers/polyaniline composites flexible electrodes

Pin Zhai[1], Ziyang Chang[1,2,*], Xinyu Zhao[1], Haiping Wang[1], Zhixin Jia[1], Lingqi Huang[1], Xiaohong Chen[1], Yahui Meng[1], Lizhen Fang[3], Yu Meng[2], Lixing Du[2], Huifang Zhao[1], Daliang Guo[1], Shangru Zhai[1,*], Lizheng Sha[1], Yonghao Ni[4,*]

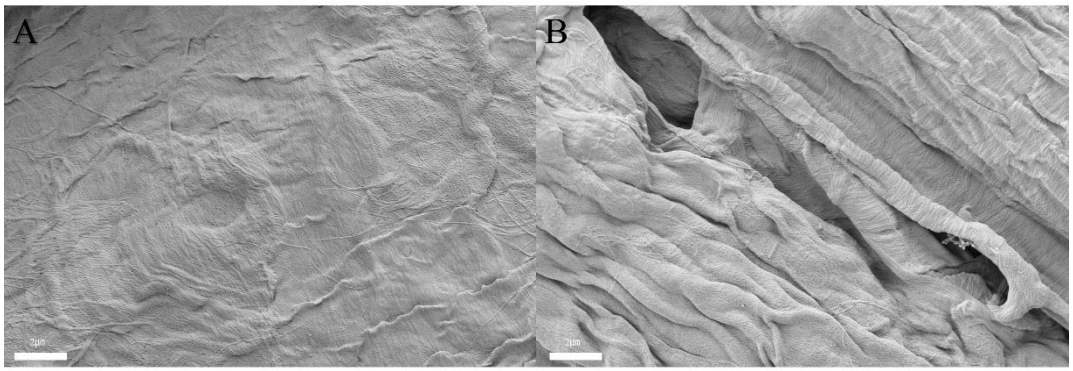
[1]Key Laboratory of Recycling and Eco-treatment of Waste Biomass of Zhejiang Province, Zhejiang University of Science and Technology, Hangzhou 310023, Zhejiang, China.

[2]Zhejiang Jinchang Special Paper Co., Ltd., Quzhou 324400, Zhejiang, China.

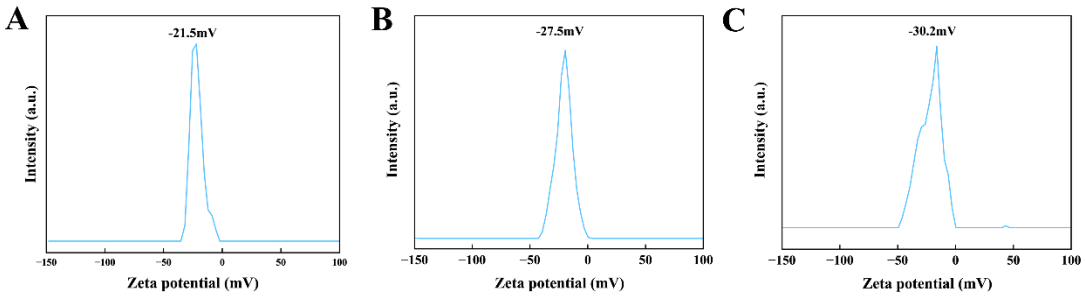
[3]Zhejiang Jiaweikang Special Paper Co., Ltd., Quzhou 324400, Zhejiang, China.

[4]Limerick Pulp and Paper Centre, University of New Brunswick, Fredericton E3B 5A3, Canada.

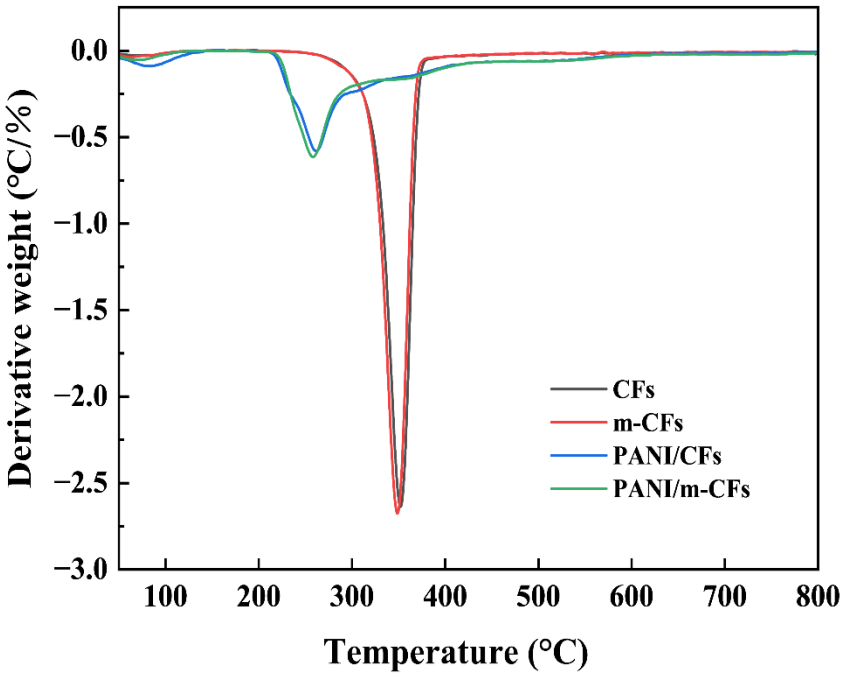
[*]**Correspondence to:** Dr. Ziyang Chang, Key Laboratory of Recycling and Eco-treatment of Waste Biomass of Zhejiang Province, Zhejiang University of Science and Technology, Hangzhou 310023, Zhejiang, China; Zhejiang Jinchang Special Paper Co., Ltd., Quzhou 324400, Zhejiang, China. E-mail: zychang@zust.edu.cn; Prof. Shangru Zhai, Key Laboratory of Recycling and Eco-treatment of Waste Biomass of Zhejiang Province, Zhejiang University of Science and Technology, Hangzhou 310023, Zhejiang, China. E-mail: zhaisr@zust.edu.cn; Prof. Yonghao Ni, Limerick Pulp and Paper Centre, University of New Brunswick, Fredericton E3B 5A3, Canada. E-mail: yonghao@unb.ca



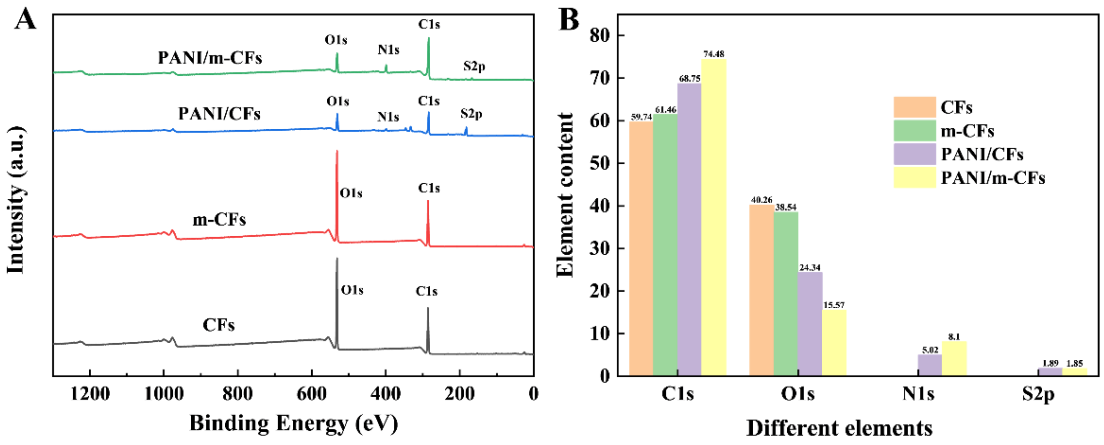
Supplementary Figure 1. Morphology of the cellulose surface before and after treatment. (A) Untreated cellulose; (B) Enzyme-treated cellulose.



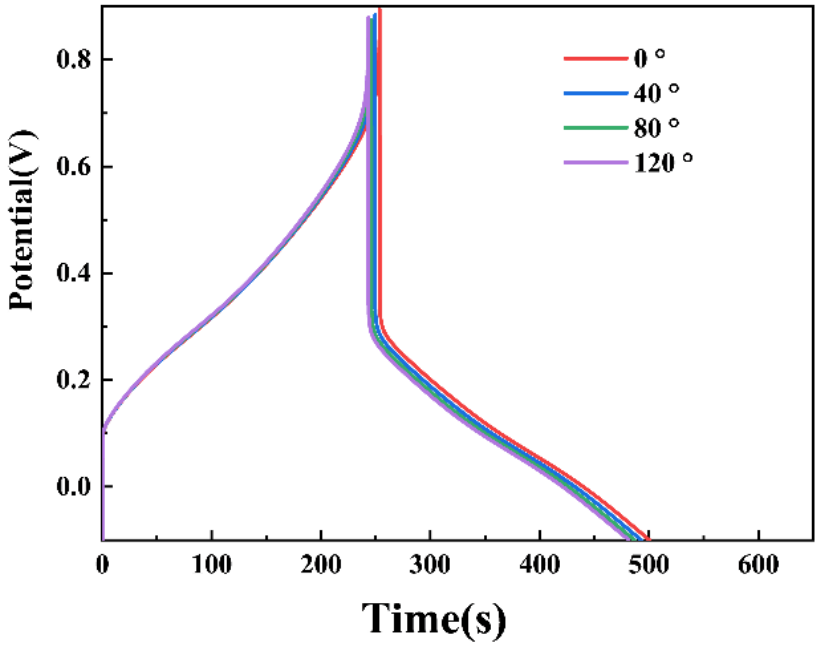
Supplementary Figure 2. Zeta potential of various samples: (A) Zeta potential distribution curve of Sample 1; (B) Zeta potential distribution curve of Sample 2; (C) Zeta potential distribution curve of Sample 4.



Supplementary Figure 3. DTG curves of samples.



Supplementary Figure 4. XPS survey spectra and elemental contents. (A) XPS survey spectra of CFs, m-CFs, PANI/CFs and PANI/m-CFs; (B) corresponding elemental content histogram.



Supplementary Figure 5. GCD curves of the electrode recorded at bending angles of 0°, 40°, 80°, and 120°.

Determination of cellulose yield and mass loss

The cellulose yield and mass loss after bio-etching were calculated based on the oven-dry masses of cellulose fibers before and after enzymatic treatment according to the following equations:

$$Y(\%)=\frac{M_B}{M_A}\times 100 \quad \text{(S1)}$$

$$\mathrm{ML}=\frac{M_A\text{-}M_B}{M_A}\times 100\% \quad \text{(S2)}$$

where M_A and M_B represent the oven-dry masses of cellulose fibers before and after enzymatic treatment, respectively. Three independently prepared samples were measured for each bio-etching condition, and the results are expressed as mean ± SD (n = 3)**.**

Supplementary Table 1. Cellulose yield and mass loss after different bio-etching treatments

Sample	**Bio-etching time (min)**	**Cellulose yield (%)**	**Mass loss (%)**
Sample 1	0	100	0
Sample 2	5	99.7 ± 0.3	0.3 ± 0.3
Sample 3	10	99.2 ± 0.4	0.8 ± 0.4
Sample 4	20	98.6 ± 0.3	1.4 ± 0.3

Supplementary Table 2. Gravimetric quantification of the PANI–SSA active phase and physical parameters of the paper-based electrodes

Sample	Rep.	M_0 (g)	M_1 (g)	ΔM_{active} (g)	LA (mg/cm^2)	w_{active} (wt%)	Electrode mass (g)	Thickness (mm)	Grammage (mg/cm^2)	m_{active} (mg/cm^2)	Mean ± SD (mg/cm^2)
Sample 1	1	0.0818	0.0986	0.0168	1.337	17.04	0.01124	0.14	7.49	1.28	1.08 ± 0.18
	2	0.0818	0.0945	0.0127	1.011	13.44	0.01158	0.13	7.72	1.04	
	3	0.0818	0.0921	0.0103	0.820	11.18	0.01092	0.13	7.28	0.81	
	4	0.0818	0.0953	0.0135	1.074	14.17	0.01128	0.14	7.52	1.07	
	5	0.0818	0.0973	0.0155	1.233	15.93	0.01118	0.14	7.45	1.19	
Sample 2	1	0.0818	0.1021	0.0203	1.615	19.88	0.01187	0.15	7.91	1.57	1.77 ± 0.15
	2	0.0818	0.1035	0.0217	1.727	20.97	0.01222	0.15	8.15	1.71	
	3	0.0818	0.1031	0.0213	1.695	20.66	0.01237	0.15	8.25	1.70	
	4	0.0818	0.1077	0.0259	2.061	24.05	0.01208	0.16	8.05	1.94	
	5	0.0818	0.1076	0.0258	2.053	23.98	0.01196	0.16	7.97	1.91	
Sample 3	1	0.0818	0.1203	0.0385	3.064	32.00	0.01442	0.19	9.61	3.08	2.93 ± 0.16

	2	0.0818	0.1187	0.0369	2.936	31.09	0.01389	0.18	9.26	2.88	
	3	0.0818	0.1214	0.0396	3.151	32.62	0.01421	0.19	9.47	3.09	
	4	0.0818	0.1182	0.0364	2.897	30.80	0.01428	0.17	9.52	2.93	
	5	0.0818	0.1145	0.0327	2.602	28.56	0.01415	0.17	9.43	2.69	
Sample 4	1	0.0818	0.1082	0.0264	2.101	24.40	0.01321	0.17	8.81	2.15	2.04 ± 0.19
	2	0.0818	0.1078	0.0260	2.069	24.12	0.01289	0.18	8.59	2.07	
	3	0.0818	0.1087	0.0269	2.141	24.75	0.01237	0.18	8.25	2.04	
	4	0.0818	0.1098	0.0280	2.228	25.50	0.01304	0.18	8.69	2.22	
	5	0.0818	0.1021	0.0203	1.615	19.88	0.01298	0.16	8.65	1.72	

Notes: The 0.5 g sample refers to the cellulose pulp with a moisture content of 83.64%, corresponding to an oven-dry cellulose mass of 0.0818 g. M_0, oven-dry cellulose mass before polymerization; M_1, dry composite mass after polymerization, washing, and drying to constant mass; $\Delta M_{active} = M_1 - M_0$; LA, PANI:SSA active-phase areal loading; w_{active}, PANI:SSA active-phase mass fraction. The precursor disk diameter was 4.0 cm (A = 12.566 cm^2). Electrode specimens had a total area of 1.00 cm^2. The active-phase mass within this area is reported as mean ± SD (n = 5).

Determination of titratable carboxyl groups

The titratable carboxyl group content of cellulose fibers before and after bio-etching was determined by conductometric titration. Briefly, 0.1 g of dried cellulose fibers was dispersed in 15 mL of 0.01 M HCl solution and stirred magnetically for 20 min to convert ionized carboxyl groups into their protonated form. Subsequently, 35 mL of deionized water was added to dilute the suspension, and the initial conductivity was recorded. The suspension was then titrated with 0.01 M NaOH solution. During titration, 0.1 mL of NaOH solution was added at each interval, and the conductivity was recorded after each addition until the neutralization process was completed. The titratable carboxyl group content was calculated based on the amount of NaOH consumed during the neutralization region. Three independent measurements were performed for each sample, and the results are expressed as mean ± SD (n = 3).

$$C_{COOH}=\frac{C_{NaOH}\times V_{NaOH}\times 1000}{m} \quad \text{(S3)}$$

Where C_{COOH} is the titratable carboxyl group content (mmol/g), C_{NaOH} is the NaOH concentration (mol/L), V_{NaOH} is the consumed NaOH volume (L), and m is the oven-dry mass of cellulose fibers (g).

Supplementary Table 3. Quantification of accessible titratable carboxyl groups on cellulose fibers before and after enzymatic bio-etching

Sample	Bio-etching time (min)	Titratable carboxyl group content (mmol/g)
Sample 1	0	0.0446 ± 0.0067
Sample 3	10	0.0563 ± 0.0019

The crystallinity index (CI) was calculated using the Segal method according to the following equation:

$$CI(\%)=\frac{I_{002}-I_{am}}{I_{002}}\times 100 \quad \text{(S4)}$$

Where I_{002} represents the maximum intensity of the (002) diffraction peak of cellulose I, and I_{am} represents the diffraction intensity of the amorphous region.

Supplementary Table 4. Crystallinity index of cellulose fibers before and after bio-etching calculated using the Segal method

Sample	$2\theta_{002}$ (°)	I_{002}	$2\theta_{am}$ (°)	I_{am}	Crystallinity index (%)
CFs	22.35	6792.22	17.99	1350.29	80.12
m-CFs	22.52	4723.2	18.00	910.93	80.71

Note: The crystallinity index was calculated using the Segal equation. The results indicate that bio-etching treatment maintained the cellulose I crystalline structure.

Supplementary Table 5. Equivalent-circuit fitting parameters and fitting quality for EIS spectra of the untreated and bio-etched electrodes

Parameter	Sample 1	Error (%)	Sample 3	Error (%)
R_s (Ω)	2.39	0.73	2.39	0.52
R_{ct} (Ω)	2.73	1.51	1.56	1.68
W-R (Ω)	3.18	7.19	1.23	9.10
W-T	0.94	12.33	0.63	15.61
W-P	0.35	2.23	0.34	1.90
CPE-T ($\times 10^{-3}$)	0.83	9.85	1.59	10.90
CPE-P	0.64	1.66	0.63	1.92
χ^2 ($\times 10^{-4}$)	8.72	—	6.57	—
Sum of squares ($\times 10^{-2}$)	10.03	—	7.55	—

Notes: All parameters listed above were obtained from the fully free ZView fits, so that parameter uncertainties could be evaluated. Error (%) values are the relative fitting errors reported by ZView. EIS measurements were conducted at the open-circuit potential from 10^5 to 0.1 Hz using a 5 mV sinusoidal perturbation. Interpretation: R_s is the series resistance, R_{ct} is the charge-transfer resistance, CPE represents the non-ideal interfacial capacitive response, and W describes the diffusion-related impedance.

Supplementary Table 6. Comparison of electrochemical testing conditions and areal capacitance of PANI-based electrodes reported in Refs. 1-5 and the present work

Electrode material	Electrolyte	Test configuration	Method	Test condition	Areal capacitance (mF cm^{-2})	PANI loading/content	Ref.
CNTF/PANi	—	Three-electrode	GCD	1 mA cm^{-2}	2035.6	3.63 mg cm^{-2}	[1]
TOCN-SCNT-PANI	1 M H_2SO_4	Not explicitly specified	GCD	1 mA cm^{-2}	1786	—	[2]
Cellulose/GO/PANI	1 M H_2SO_4	Three-electrode	GCD	1.0 mA cm^{-2}	1218	~15 wt%	[3]
PANI/Ti	1 M H_2SO_4	Three-electrode	GCD	2 mA cm^{-2}	1174	—	[4]
PANI/NF	3 M KOH	Three-electrode	CV	10 mV s^{-1}	1445	—	[5]
PANI/m-CFs	1 M H_2SO_4	Three-electrode	GCD	1 mA cm^{-2}	2098	2.93 mg cm^{-2}	This work

REFERENCES

1. Zhou, H.; Ren, Z.; Ou, T.; et al. Template-free water splitting preparation of carbon nanotube foam for high-efficiency charge storage and electromagnetic interference shielding. *J. Power Sources* **2025**, *644*, 237096.[DOI:10.1016/j.jpowsour.2025.237096].
2. Hu, Y.; Zhan, Y.; Xu, M.; et al. One-step preparation of flexible nanocellulose-based composite hydrogel supercapacitors with high specific capacitance. *Compos. Sci. Technol.* **2022**, *230*, 109725.[DOI:10.1016/j.compscitech.2022.109725].
3. Li, Y.; Xia, Z.; Gong, Q.; et al. Green Synthesis of Free Standing Cellulose/Graphene Oxide/Polyaniline Aerogel Electrode for High-Performance Flexible All-Solid-State Supercapacitors. *Nanomaterials* **2020**, *10*, 1546.[DOI:10.3390/nano10081546].
4. Hossain, M. S.; Kabir, M. H.; Shaikh, M. A. A.; et al. Development of a high-capacitance flexible supercapacitor with enhanced cycling stability based on nanotubular polyaniline-modified titanium sheet. *Mater. Chem. Phys.* **2024**, *322*, 129586.[DOI:10.1016/j.matchemphys.2024.129586].
5. Shah, S. S.; Das, H. T.; Barai, H. R.; et al. Boosting the Electrochemical Performance of Polyaniline by One-Step Electrochemical Deposition on Nickel Foam for High-Performance Asymmetric Supercapacitor. *Polymers* **2022**, *14*, 270.[DOI:10.3390/polym14020270].